

# Investigation and FDTD Analysis of UWB Microstrip Antenna with Dual Narrow Band-Notched Characteristic

Nasser Ojaroudi<sup>1</sup>, Mehdi Mehranpour<sup>1</sup>, Yasser Ojaroudi<sup>2</sup>, and Sajjad Ojaroudi<sup>2</sup>

<sup>1</sup> Young Researchers and Elite Club  
Islamic Azad University, Ardabil Branch, Ardabil, Iran  
n.ojaroudi@yahoo.com, mehranpour.mehdi@gmail.com

<sup>2</sup> Young Researchers and Elite Club  
Islamic Azad University, Germe Branch, Germe, Iran  
y.ojaroudi@iaugerme.ac.ir, s.ojaroudi.p@yahoo.com

**Abstract** — In this manuscript, a novel design of Ultra-Wideband (UWB) monopole antenna with dual narrow band-stop performance is proposed. In this design, by using inverted T-shaped slit and T-shaped parasitic structure in the ground plane, additional resonances are excited and much wider impedance bandwidth can be produced; especially at the higher band. In order to generate single and dual band-notched characteristics, we use a pair of protruded E-shaped strips inside the square-ring radiating patch. The measured results reveal that the presented dual band-notched monopole antenna offers a very wide bandwidth from 3.01 GHz to 12.8 GHz with two narrow notched bands, covering 5.2/5.8 GHz to suppress interferences from Wireless Local Area Network (WLAN) system. To verify the validation of proposed antenna, Finite-Difference Time-Domain (FDTD) analysis is investigated. Good return loss, antenna gain and radiation pattern characteristics are obtained in the frequency band of interest. The antenna imposes negligible effects on the transmitted pulses.

**Index Terms** — Dual narrow notch bands, FDTD analysis, microstrip antenna, UWB applications.

## I. INTRODUCTION

After allocation of the frequency band from 3.1 to 10.6 GHz for the commercial use of Ultra-Wideband (UWB) systems by the Federal Communication Commission (FCC) [1], UWB systems have received phenomenal gravitation in

wireless communication. Designing an antenna to operate in the UWB band is quite a challenge because it has to satisfy the requirements, such as ultra wide impedance bandwidth, omni-directional radiation pattern, constant gain, high radiation efficiency, constant group delay, low profile, easy manufacturing, etc. [2]. In UWB communication systems, one of key issues is the design of a compact antenna while providing wideband characteristic over the whole operating band. Consequently, a number of microstrip antennas with different geometries have been experimentally characterized [3-6].

In [3], a compact hexagonal structure is used to enhance the impedance bandwidth. Based on Defected Ground Structure (DGS) and Electromagnetic Coupling Theory (ECT), slot and parasitic structures are used to excite more resonances in [4]. A novel CPW-fed E-shaped slot antenna which provides a wide usable fractional bandwidth of more than 115% is reported in [5]. Moreover, other strategies to improve the impedance bandwidth which do not involve a modification of the geometry of the planar antenna have been investigated [6-7].

There are many narrowband communication systems which severely interfere with the UWB communication system, such as the Wireless Local Area Network (WLAN) for IEEE 802.11a operating in 5.15-5.35 and 5.725-5.825 GHz bands. Therefore, UWB antennas with band-notched characteristic to filter the potential interference are desirable. Nowadays, to mitigate

this effect, many UWB antennas with various band-notched properties have developed [8-9].

All of the above methods are used for rejecting a single band of frequencies. However, to effectively utilize the UWB spectrum and to improve the performance of the UWB system, it is desirable to design the UWB antenna with dual band rejection. It will help to minimize the interference between the narrow band systems with the UWB system. Some methods are used to obtain the dual band rejection in the literature [10-14].

In this paper, a new design of 5.2/5.8 GHz dual narrow band-notched printed monopole antenna with multi-resonance performance is presented. The proposed antenna consists of square-ring radiating patch with a pair of protruded E-shaped strips, and modified ground plane with inverted T-shaped slit and T-shaped parasitic structure. The proposed antenna has a small size of  $12 \times 18 \text{ mm}^2$ .

## II. ANTENNA DESIGN

Configuration of the proposed monopole antenna fed by a microstrip line is shown in Fig. 1.

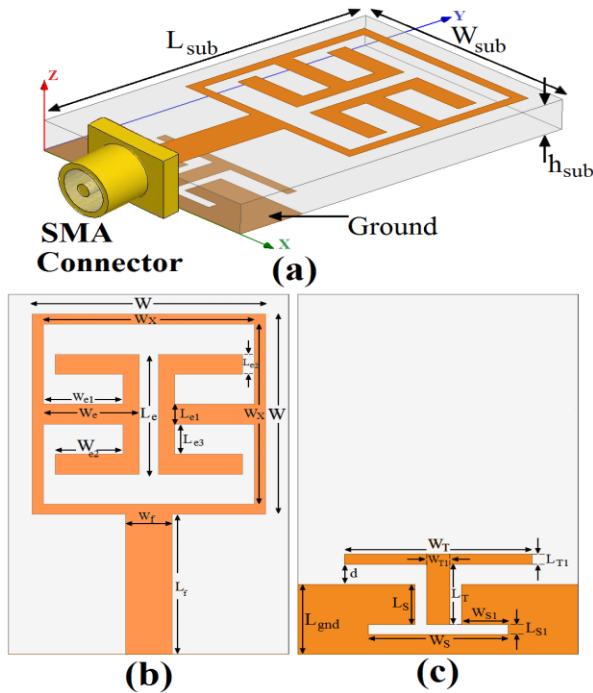


Fig. 1. Geometry of the proposed antenna: (a) side view, (b) top layer, and (c) bottom layer.

The dielectric substance (*FR4*) with thickness of 1.6 mm with relative permittivity of 4.4 and loss tangent 0.018 is chosen as substrate to facilitate printed circuit board integration. The square patch has a width  $W$ . The radiating patch is connected to a feed line with width of  $W_f$  and length of  $L_f$ . The width of the microstrip feed-line is fixed at 2 mm, as shown in Fig. 1. The proposed antenna is connected to a 50- $\Omega$  SMA connector for signal transmission.

This work started by choosing the dimensions of the designed antenna. Hence, the essential parameters for the design are:  $f_0=4.5$  GHz (first resonance frequency),  $\epsilon_r=4.4$  and  $h_{sub}=0.8$  mm. The dimensions of the patch along its length have now been extended on each end by a distance  $\Delta L$ , which is given as:

$$\Delta L = 0.412 h_{sub} \frac{(\epsilon_{eff} + 0.3) \left( \frac{W_{sub}}{h_{sub}} + 0.264 \right)}{(\epsilon_{eff} - 0.258) \left( \frac{W_{sub}}{h_{sub}} + 0.8 \right)}, \quad (1)$$

where  $h_{sub}$  is the height of dielectric,  $W_{sub}$  is the width of the microstrip monopole antenna and  $\epsilon_{r\text{eff}}$  is the effective dielectric constant. Then, the effective length ( $L_{eff}$ ) of the patch can be calculated as follows:

$$L_{eff} = L + 2\Delta L. \quad (2)$$

For a given resonant frequency  $f_0$ , the effective length is given as:

$$L_{eff} = \frac{C}{2f_0 \sqrt{\epsilon_{reff}}}. \quad (3)$$

For a microstrip antenna, the resonance frequency for any  $TM_{mn}$  mode is given by as:

$$\epsilon_{eff} = \frac{(\epsilon_r + 1)}{2} + \frac{(\epsilon_r - 1)}{2} \left[ 1 + 12 \frac{h_{sub}}{W_{sub}} \right]^{-\frac{1}{2}}. \quad (4)$$

The width  $W_{sub}$  of microstrip antenna is given:

$$W_{sub} = \frac{C}{2f_0 \sqrt{(\epsilon_r + 1)}}. \quad (5)$$

The last and final step in the design is to choose the length of the resonator and the band-stop filter elements. In this design, the optimized length  $L_{resonance}$  is set to resonate at  $0.25\lambda_{resonance}$ , where  $L_{resonance1} = W_{S1} + L_S + 0.5L_{S1}$  and  $L_{resonance2} = 0.5(L_{T1} + d) + 0.5W_T - W_{T1}$ .  $\lambda_{resonance1}$  and  $\lambda_{resonance2}$  corresponds to first extra resonance frequency (11

GHz) and second extra frequency (12 GHz), respectively.

In addition, to create a desired dual frequency band-stop characteristic, a pair of protruded E-shaped strips are used inside square-ring radiating patch. At the notched frequencies, the current flows are more dominant around the T-shaped and C-shaped structures, and they are oppositely directed between the embedded structures and the radiating stub. As a result, the desired high attenuation near the notched frequency can be produced. Also, the optimized length  $L_{\text{notch}}$  is set to band-stop resonate at  $0.5\lambda_{\text{notch}}$ , where  $L_{\text{notch1}}=W_{e1}+L_{e3}+0.5(L_e+L_{e2})$ , and  $L_{\text{notch2}}=W_e+L_{e1}+0.5L_e$ .  $\lambda_{\text{notch1}}$  and  $\lambda_{\text{notch2}}$  corresponds to first band-notched frequency (3.9 GHz) and second band-notched frequency (5.5 GHz), respectively. The final values of proposed design parameters are specified in Table 1.

Table 1: Final dimensions of the antenna

Parameter	$W_{\text{sub}}$	$L_{\text{sub}}$	$h_{\text{sub}}$	$W_f$	$L_f$	$W$
(mm)	12	18	1.6	2	7	10
Parameter	$W_S$	$L_S$	$W_{S1}$	$L_{S1}$	$W_T$	$L_T$
(mm)	6	2	2	0.5	8	3
Parameter	$W_{T1}$	$L_{T1}$	$W_e$	$L_e$	$W_{e1}$	$L_{e1}$
(mm)	1	0.5	4	6	3.5	1
Parameter	$W_{e2}$	$L_{e2}$	$W_X$	$L_{e3}$	$d$	$L_{\text{gnd}}$
(mm)	3	1	9	1.5	1	3.5

### III. RESULTS AND DISCUSSIONS

In this section, the proposed microstrip monopole antenna with various design parameters was constructed. The parameters of the proposed antenna are studied by changing one parameter at a time and fixing the others. The analysis and performance of the proposed antenna is explored by using Ansoft simulation software High-Frequency Structure Simulator (HFSS) [15], for better impedance matching.

#### A. UWB antenna with multi-resonance characteristic

The configuration of various structures used for simulation studies were shown in Fig. 2. Return loss characteristics for the ordinary monopole antenna [Fig. 2 (a)], antenna with an inverted T-shaped slit in the ground plane [Fig. 2 (b)], and the antenna with inverted T-shaped slit and T-shaped conductor-backed plane [Fig. 2 (c)]

are compared in Fig. 3.

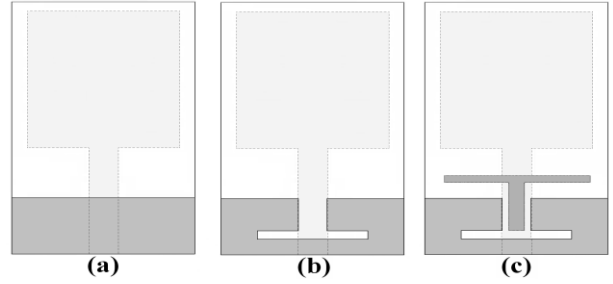


Fig. 2. (a) Ordinary monopole antenna, (b) antenna with an inverted T-shaped slit, and (c) antenna with inverted T-shaped slit and T-shaped parasitic structure.

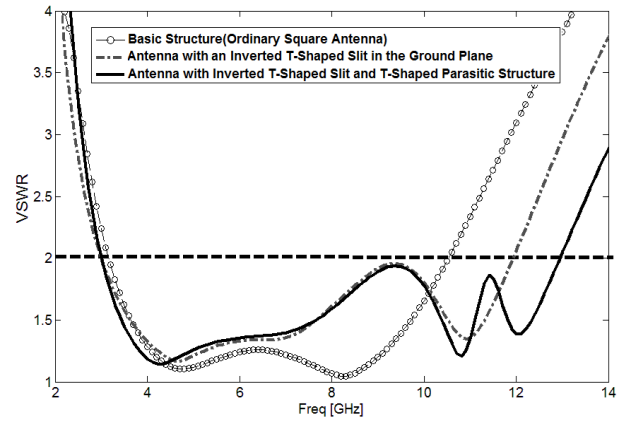


Fig. 3. Simulated return loss characteristics for the various antenna structures shown in Fig. 2.

As seen, the upper frequency bandwidth is significantly affected by using T-shaped structures in the ground plane. By using these modified elements, additional third (11 GHz) and fourth (12 GHz) resonances are excited, respectively. By using these modified structures, the usable upper frequency of the antenna is extended from 10.4 GHz to 12.8 GHz, which provides a wide usable fractional bandwidth of more than 125%.

Moreover, the input impedance of the various structures of the multi-resonance antenna on a Smith-Chart is shown in Fig. 4. The multi-resonance behavior is mainly due to the change of surface current path by changing the dimensions of the pair of T-shaped structures. In order to know the phenomenon behind the additional resonances performance, simulated current

distributions on the ground plane for the proposed antenna at 11 GHz and 12 GHz are presented in Fig. 5. It can be observed in Fig. 5 (a), that the current concentrated on the edges of the interior and exterior of the inverted T-shaped slit at 11 GHz. As shown in Fig. 5 (b), at the fourth resonance frequency the current flows are more dominant around of the T-shaped parasitic structure [8-9].

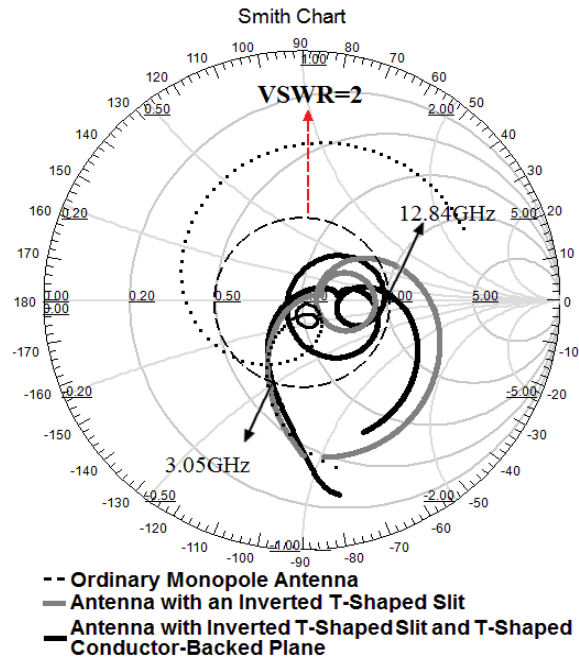


Fig. 4. Simulated input impedance results on a Smith Chart of various structures shown in Fig. 2.

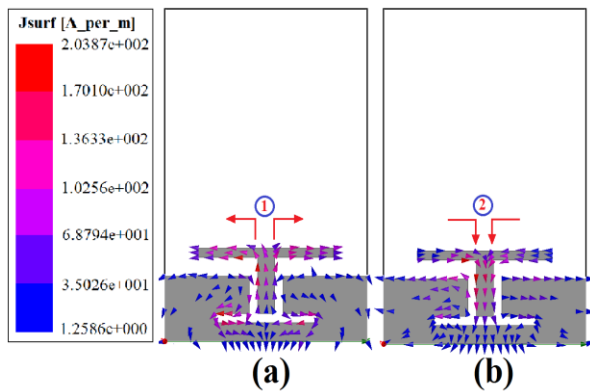


Fig. 5. Simulated surface current distributions in the ground plane for the proposed antenna: (a) at 11 GHz and (b) at 12 GHz.

In order to investigate the effects of the inverted T-shaped slit and T-shaped parasitic structures on the bandwidth of the proposed antenna and impedance matching, the VSWR characteristics for various slit and parasite sizes were analyzed in Figs. 6 and 7. As illustrated, four structures with different sizes of inverted T-shaped slit and T-shaped parasitic structure are shown in these figures. It is found that by using these structures with modified sizes of  $W_s = 6$  &  $W_T = 8$ , good additional resonances is excited and hence much wider impedance bandwidth with multi-resonance characteristics can be produced; which the usable upper frequency of the antenna is extended from 10.3 GHz to 12.84 GHz.

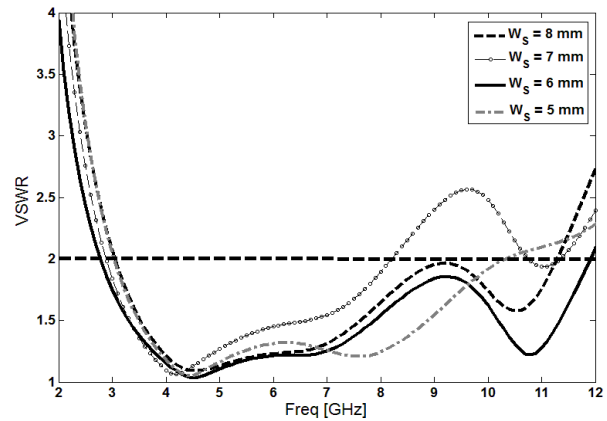


Fig. 6. Simulated VSWR characteristics for the various sizes of  $W_s$ .

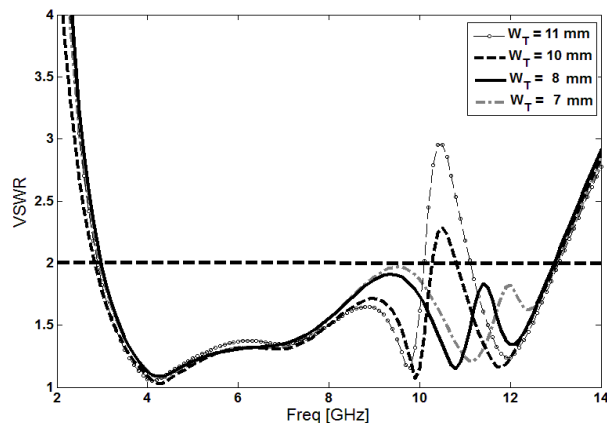


Fig. 7. Simulated VSWR characteristics for the various sizes of  $W_T$ .

## B. UWB antenna with dual narrow band-notched function

In order to generate the dual narrow band-notched characteristic, we used a pair of protruded E-shaped strips inside the square-ring radiating patch.

VSWR characteristics for antenna with a modified ground plane [Fig. 8 (a)], the antenna with modified ground plane and a protruded E-shaped strip inside square-ring radiating patch [Fig. 8 (b)], and the proposed antenna structure [Fig. 8 (c)] are compared in Fig. 9. As seen, to create a single band-notched characteristic, we use an E-shaped strip at square-ring radiating patch. Also, by adding another E-shaped strip, a good dual band-notched function is achieved.

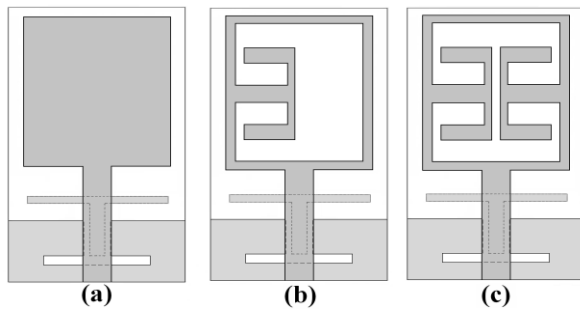


Fig. 8. (a) Antenna with modified ground plane, (b) the antenna with modified ground plane and protruded E-Shaped strip, and (c) the proposed antenna structure.

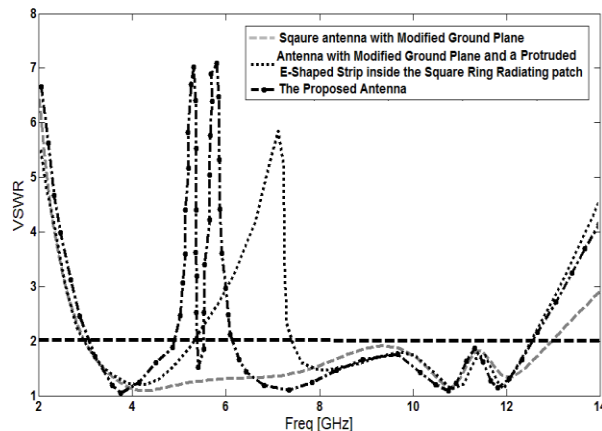


Fig. 9. Simulated VSWR characteristics for the various structures shown in Fig. 8.

In order to understand the phenomenon behind this dual band-stop performance, the simulated current distributions for the proposed antenna at the notched frequencies is presented in Fig. 10. It is found at the notched frequencies the current flows are more dominant around of the protruded E-shaped strips [10-12]. The proposed antenna with final design as shown in Fig. 11, was built and tested.

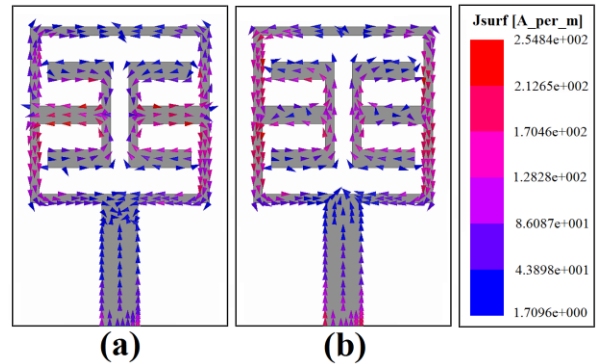


Fig. 10. Simulated surface current distributions for the proposed antenna in the radiating patch at the notched frequencies: (a) 5.2 GHz and (b) 5.8 GHz.

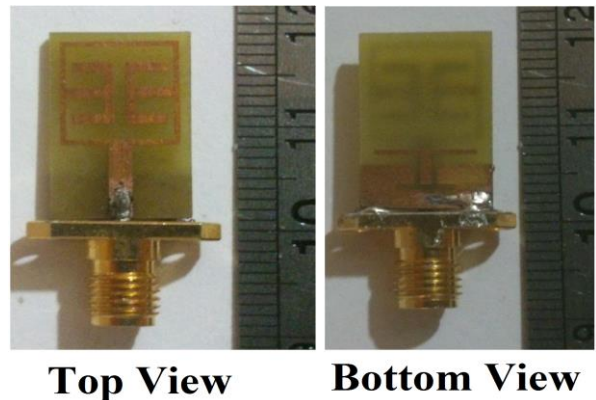


Fig. 11. Photograph of the realized antenna.

Figure 12 shows the effects of the pairs of T-shaped and E-shaped structures embedded at the proposed antenna configuration on the maximum gain in comparison to the ordinary square antenna without them. As seen, the ordinary square antenna has a gain that is low at 3 GHz and increases with frequency. It can be observed that

by using the pair of protruded E-shaped strips inside the square-ring radiating patch, the sharp decreases of maximum gain and the notched frequency bands (5.2 and 5.8 GHz) can be created. For other frequencies outside the notched frequencies, the antenna gain with the filters is similar to those without them [13].

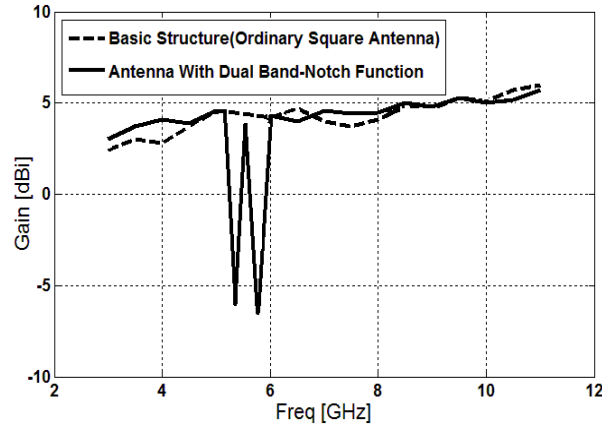


Fig. 12. Measured maximum gain of the proposed antenna in compared with the ordinary structure.

Figure 13 illustrates the FDTD computed and measured radiation patterns, including the co-polarization and cross-polarization in the H-plane ( $x$ - $z$  plane) and E-plane ( $y$ - $z$  plane). The main purpose of the radiating patterns is to demonstrate that the antenna actually radiates over a wide frequency band. It can be seen that the radiation patterns in  $x$ - $z$  plane are nearly omni-directional for the three frequencies. The radiation patterns on the  $y$ - $z$  plane are like a small electric dipole leading to bidirectional patterns in a very wide frequency band [13-14]. The comparison between measured and numerically computed radiation patterns are well within the acceptable limits.

Table 2 summarizes the proposed antenna and the previous designs [10-14]. As seen, the proposed antenna has a compact size with very wide bandwidth in compared to the pervious works. In addition, the proposed antenna has good omni-directional radiation patterns with low cross-polarization level, even at higher and upper frequencies. Also, the antenna imposes negligible effects on the transmitted pulses and has acceptable gain levels in the operation bands [16].

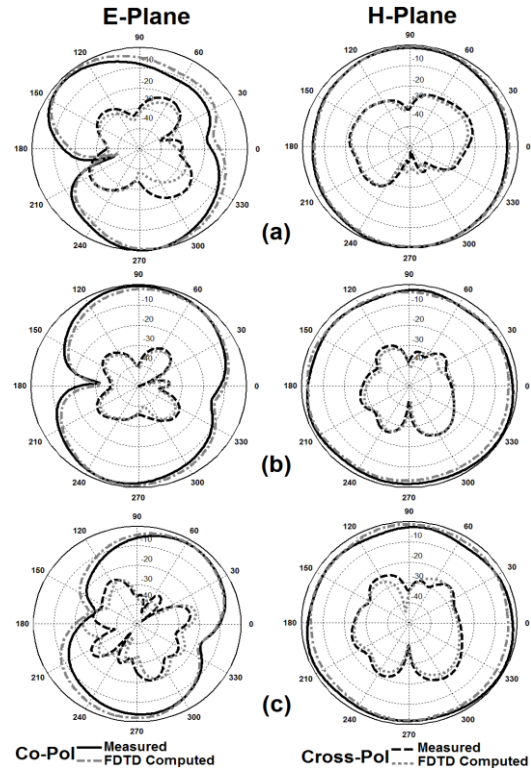


Fig. 13. The FDTD computed measured and radiation patterns of the proposed antenna at: (a) 4.2 GHz, (b) 8 GHz, and (c) 11.5 GHz.

Table 2: Comparison of previous designs with the proposed antenna

Ref.	FBW (%)	Dimension
[10]	1.8-10.5 GHz (140%)	30 mm×35 mm
[11]	2.4-10.1 GHz (120%)	28 mm×33 mm
[12]	2.8-12.0 GHz (124%)	24 mm×24 mm
[13]	3.1-10.6 GHz (109%)	16 mm×25 mm
[14]	3.0-12.0 GHz (121%)	21 mm×36 mm
<i>This Work</i>	<i>3.0-12.8 GHz (125%)</i>	<i>12 mm×18 mm</i>

#### IV. NUMERICAL RESULTS AND TIME-DOMAIN ANALYSIS

##### A. Numerical results

In this section, the results using FDTD method are derived for the proposed antenna and are compared with the simulated (HFSS) ones. The space steps used in Cartesian coordination are  $\Delta x = 0.25mm$ ,  $\Delta y = 0.25mm$ ,  $\Delta z = 0.25mm$ , and

the total mesh dimensions are  $58 \times 110 \times 25$  in  $x$ ,  $y$  and  $z$  directions, respectively. The antenna patch (Fig. 1) is thus  $40\Delta x \times 40\Delta y$ . The length of the microstrip line from the source plane to the edge of the antenna is  $150\Delta y$ , and the reference plane for port 1 is  $28\Delta y$  from the edge of the patch. The microstrip line width is modeled as  $8\Delta x$ . The time step used, according to Courant's condition is  $\Delta t = 0.66 ps$ .

The launched wave has approximately unit amplitude and is Gaussian in time given by:

$$E_z(t) = e^{-(t-t_0)^2/T^2}. \quad (6)$$

The wave's half-width is  $T = 4\Delta t$  and the time delay  $t_0$  is set to be  $6T$ , so the Gaussian will start at approximately 0; also, similar in [17], the magnetic wall source is used to minimize the source distortion. The spatial distribution of  $E_z(x, y, t)$  just beneath the microstrip at 450, 1000, 1200 and 1800 time steps is shown in Fig. 14, where the Gaussian pulse and subsequent propagation on the antenna are observed. Also, the incident, total and reflected voltages at the reference plane are illustrated in Fig. 15 for all time steps.

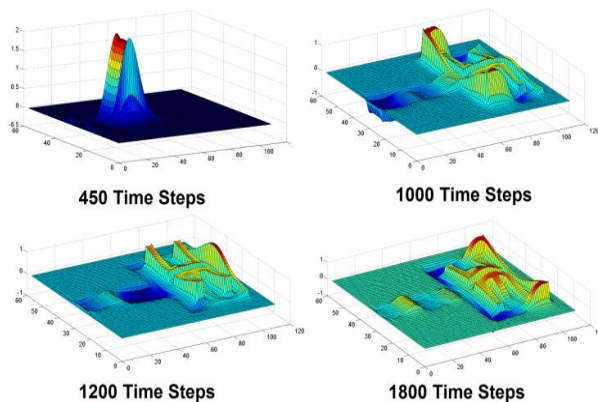


Fig. 14. The spatial distribution of  $E_z(x, y, t)$  just beneath the microstrip at 450, 1000, 1200 and 1800 time steps.

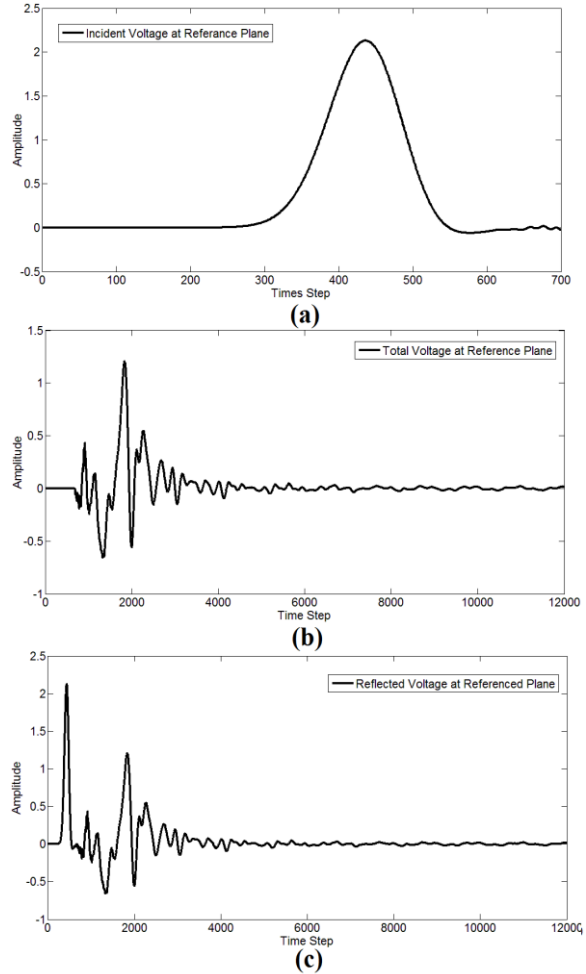


Fig. 15. (a) Incident voltage, (b) total voltage, and (c) reflected voltage at the reference plane:  $50 \Delta y$  from the edge of the patch.

Measured and simulated VSWR characteristic of the proposed antenna which was calculated using FDTD and HFSS, were shown in Fig. 16. The fabricated antenna has the frequency band of 3.01 to over 12.8 GHz. Also, the frequency bands of 5.15-5.35 and 5.725-5.825 GHz are notched with maximum VSWRs more than 6.5, which is sufficient and deep enough to avoid the possible interference between UWB and WLAN systems.

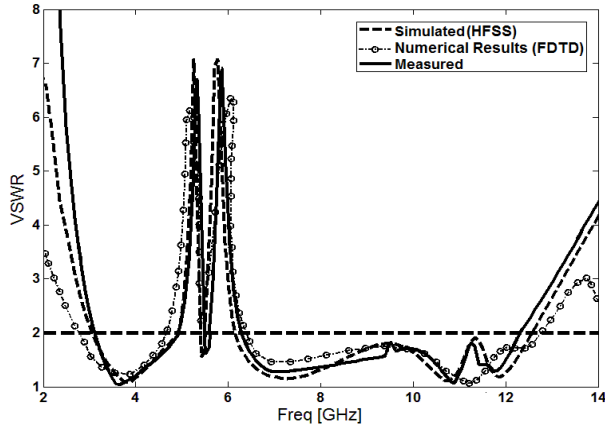


Fig. 16. Measured, simulated and FDTD computed VSWR characteristics for the antenna.

**B. Time-domain analysis**

In telecommunications systems, the correlation between Transmitted (TX) and Received (RX) signals is evaluated using the fidelity factor (7):

$$F = \text{Max}_\tau \left| \frac{\int_{-\infty}^{+\infty} s(t)r(t - \tau) dt}{\sqrt{\int_{-\infty}^{+\infty} s(t)^2 dt \cdot \int_{-\infty}^{+\infty} r(t)^2 dt}} \right|, \quad (7)$$

where  $s(t)$  and  $r(t)$  are the TX and RX signals, respectively.

Higher values of  $F$  prove a good correlation between the RX and TX signals. For impulse radio in UWB communications, it is necessary to have a high degree of correlation between the TX and RX signals to avoid losing the modulated information. However, for most other telecommunication systems, the fidelity parameter is not that relevant. In order to evaluate the pulse transmission characteristics of the proposed antenna, two configurations (side-by-side and face-to-face orientations) were chosen. The transmitting and receiving antennas were placed in a  $d = 250\text{mm}$  distance from each other. As shown in Fig. 17, although the received pulses in each of the two orientations are broadened, a relatively good similarity exists between the RX and TX pulses; especially in the face-to-face orientation. Using (2), the fidelity factor for face-to-face and side-by-side configurations was obtained equal to 0.81 and 0.79, respectively. The pulse transmission results are obtained using CST [19].

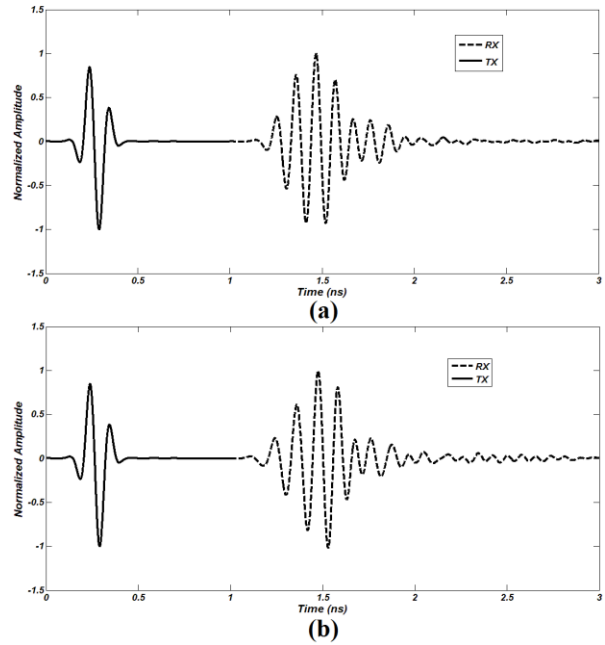


Fig. 17. Pulse transmission results: (a) side-by-side view and (b) face-to-face view.

**V. CONCLUSION**

A novel design of multi-resonance monopole antenna with dual band-notched function has been presented. The proposed antenna can operate from 3 to 12.8 GHz with two rejection bands around 4.9-5.3 GHz and 5.5-6.2 GHz, covering 5.2/5.8 GHz WLAN systems. Simulated and experimental results show that the proposed antenna could be a good candidate for UWB applications.

**REFERENCES**

- [1] "FCC news release," *FCC NEWS (FCC 02-48)*, February 14, 2002.
- [2] H. Schantz, "The art and science of ultra-wideband antennas," *Artech House*, 2005.
- [3] M. R. Ghaderi and F. Mohajeri, "A compact hexagonal wide slot antenna with microstrip-fed for UWB application," *IEEE Antennas and Wireless Propag. Lett.*, vol. 10, pp. 682-685, 2011.
- [4] N. Ojaroudi, "Design of ultra-wideband monopole antenna with enhanced bandwidth," *21<sup>st</sup> Telecommunications Forum, TELFOR 2013*, Belgrade, Serbia, pp. 1043-1046, November 27-28, 2013.
- [5] A. Dastranj and H. Abiri, "Bandwidth enhancement of printed e-shaped slot antennas fed by CPW and microstrip line," *IEEE Trans. Antenna Propag.*, vol. 58, pp. 1402-1407, 2010.

- [6] N. Ojaroudi, "A new design of koch fractal slot antenna for ultra-wideband applications," *21<sup>st</sup> Telecommunications Forum, TELFOR 2013*, Belgrade, Serbia, pp. 1051-1054, November 27-28, 2013.
- [7] A. Dastranj and H. Abiri, "Bandwidth enhancement of printed e-shaped slot antennas fed by CPW and microstrip line," *IEEE Trans. Antenna Propag.*, vol. 58, pp. 1402-1407, 2010.
- [8] N. Ojaroudi, "Application of protruded strip resonators to design an UWB slot antenna with WLAN band-notched characteristic," *Progress in Electromagnetics Research C*, vol. 47, pp. 111-117, 2014.
- [9] N. Ojaroudi, "Small microstrip-fed slot antenna with frequency band-stop function," *21<sup>st</sup> Telecommunications Forum, TELFOR 2013*, Belgrade, Serbia, pp. 1047-1050, November 27-28, 2013.
- [10] Y. Zhang, W. Hong, C. Yu, Z. Q. Kuai, Y. D. Don, and J. Y. Zhou, "Planar ultra-wideband antennas with multiple notched bands based on etched slots on the patch and/or split ring resonators on the feed line," *IEEE Transactions on Antennas and Propagation*, vol. 56, pp. 3063-3068, 2008.
- [11] J. C. Ding, Z. L. Lin, Z. N. Ying, and S. L. He, "A compact ultra-wideband slot antenna with multiple notch frequency bands," *Microwave and Optical Technology Letter*, vol. 49, pp. 3056-3060, 2007.
- [12] X. L. Ma, W. Shao, and G. Q. He, "A novel dual narrow band-notched CPW-fed UWB slot antenna with parasitic strips," *Applied Computational Electromagnetics Society (ACES) Journal*, vol. 27, pp. 581-586, 2012.
- [13] L. H. Ye and Q. X. Chu, "3.5/5.5 GHz dual band notch ultra-wideband slot antenna with compact size," *Electronics Letters*, vol. 46, pp. 325-327, 2010.
- [14] K. S. Ryu and A. A. Kishk, "UWB antenna with single or dual band notches for lower WLAN band and upper WLAN band," *IEEE Trans. Antennas and Propag.*, vol. 57, pp. 3942-3950, December 2009.
- [15] Ansoft Corporation, "Ansoft high frequency structure simulation (HFSS)," ver. 13, Pittsburgh, PA, 2010.
- [16] A. Sheta, A. Mohra, and S. F. Mahmoud, "Multi-band operation of a compact h-shaped microstrip antenna," *Microwave and Optical Tech. Lett.*, vol. 35, pp. 363-367, 2002.
- [17] CST Microwave Studio, ver. 2008, "Computer simulation technology," Framingham, MA, 2008.